NEUTRON BEAM IMAGING WITH MICROMEGAS DETECTORS IN COMBINATION WITH NEUTRON TIME-OF-FLIGHT AT THE n_TOF FACILITY AT CERN

F. Belloni[1], S. Andriamonje[2], E. Berthoumieux[1], M. Calviani[2], E. Chiaveri[2], N. Colonna[3], Y. Giomataris[1], C. Guerrero[2], F. Gunsing[1], F. J. Iguaz[1], M. Kebbiri[1], J. Pancin[1], T. Papaevangelou[1], A. Tsinganis[2,4], V. Vlachoudis[2], S. Altstadt[5], J. Andrzejewski[6], L. Audouin[7], M. Barbagallo[3], V. Bécares[8], F. Bečvář[9], J. Billowes[10], V. Boccone[2], D. Bosnar[11], M. Brugger[2], F. Calviño[12], D. Cano-Ott[8], C. Carrapiço[13], F. Cerutti[2], E. Chiaveri[1,2], M. Chin[2], G. Cortés[12], M. A. Corté-Giraldo[14], M. Diakaki[4], C. Domingo-Pardo[15], I. Duran[16], N. Dzysiuk[17], C. Eleftheriadis[18], A. Ferrari[2], K. Fraval[1], S. Ganesan[19], A. R. García[8], G. Giubrone[15], M. B. Gómez-Hornillos[12], I. F. Gonçalves[13], E. González-Romero[8], E. Griesmayer[20], P. Gurusamy[19], D. G. Jenkins[21], E. Jericha[20], Y. Kadi[2], F. Käppeler[22], D. Karadimos[4], P. Koehler[23], M. Kokkoris[4], M. Krtička[9], J. Kroll[9], C. Langer[5], C. Lederer[5,24], H. Leeb[20], L. S. Leong[7], R. Losito[2], A. Manousos[18], J. Marganiec[6], T. Marítnez[8], C. Massimi[25], P. F. Mastinu[17], M. Mastromarco[3], M. Meaze[3], E. Mendoza[8], A. Mengoni[26], P. M. Milazzo[27], F. Mingrone[25], M. Mirea[28], W. Mondalaers[29], C. Paradela[16], A. Pavlik[24], J. Perkowski[6], A. Plompen[29], J. Praena[14], J. M. Quesada[14], T. Rauscher[30], R. Reifarth[5], A. Riego[12], F. Roman[2,28], C. Rubbia[2,31], R. Sarmento[13], P. Schillebeeckx[29], S. Schmidt[5], G. Tagliente[3], J. L. Tain[15], D. Tarrío[16], L. Tassan-Got[7], S. Valenta[9], G. Vannini[25], V. Variale[3], P. Vaz[13], A. Ventura[26], R. Versaci[2], M. J. Vermeulen[21], V. Vlachoudis[2], R. Vlastou[4], A. Wallner[24], T. Ware[10], M. Weigand[5], C. Weiss[20], T. J. Wright[10], P. Žugec[11]

[1] *CEA Saclay, DSM/IRFU/SPhN, Gif-sur-Yvette, France*
[2] *European Organization for Nuclear Research (CERN), Geneva, Switzerland*
[3] *Istituto Nazionale di Fisica Nucleare, Bari, Italia*
[4] *National Technical University of Athens, Athens, Greece*
[5] *Goethe Universität, Frankfurt, Germany*
[6] *Uniwersyte Łódzki, Lodz, Poland*
[7] *Centre National de la Recherche Scientifique/IN2P3, IPN, Orsay, France*
[8] *Centro de Investigaciones Energeticas Medioambientales y Tecnólgicas, Madrid, Spain*
[9] *Charles University, Prague, Czech Republic*
[10] *University of Manchester, Oxford Road, Manchester, United Kingdom*
[11] *Department of Physics, Faculty of Science, University of Zagreb, Croatia*
[12] *Universitat Politecnica de Catalunya, Barcelona, Spain*
[13] *Instituto Tecnológico e Nuclear, Instituto Superior Técnico, Universidade Técnica de Lisboa, Lisboa, Portugal*
[14] *Universidad de Sevilla, Sevilla, Spain*
[15] *Instituto de Fisica Corpuscular, CSIC-Universidad de Valencia, Spain*
[16] *Universidad de Santiago de Compostela, Santiago de Compostela, Spain*
[17] *Istituto Nazionale di Fisica Nucleare, Laboratori Nazionali di Legnaro, Legnaro, Italy*
[18] *Aristotle University of Thessaloniki, Thessaloniki, Greece*
[19] *Bhabha Atomic Research Centre, Mumbai, India*
[20] *Atominstitut, Technische Universität Wien, Austria*
[21] *University of York, Heslington, York, United Kingdom*
[22] *Karlsruhe Institute of Technology, Campus Nord, Institut für Kernphysik, Karlsruhe, Germany*
[23] *Oak Ridge National Laboratory, Oak Ridge, TN, USA*
[24] *University of Vienna, Faculty of Physics, Austria*
[25] *Dipartimento di Fisica, Università di Bologna, and Sezione INFN di Bologna, Italy*
[26] *Agenzia nazionale per le nuove tecnologie, l'energia e lo sviluppo economico sostenibile, Bologna, Italy*
[27] *Istituto Nazionale di Fisica Nucleare, Trieste, Italy*
[28] *Horia Hulubei National Institute of Physics and Nuclear Engineering, Bucharest-Magurele, Romania*
[29] *European Commission JRC, Institute for Reference Materials and Measurements, Department of Physics and Astronomy, Geel, Belgium*
[30] *University of Basel, Basel, Switzerland*
[31] *Laboratorio Nazionali del Gran Sasso, Istituto Nazionale di Fisica Nucleare, Assergi (AQ), Italy*

A bulk micromegas detector with the anode segmented in 2 orthogonal directions and equipped with a neutron/charged particle converter is employed at the neutron time-of-flight (nTOF) facility at CERN to determine the incident neutron beam profile and beam interception factor as a function of the neutron energy determined by the time of flight. Discrepancies between experimental results and simulations in the values of the beam interception factor range up to 12 % and are to be ascribed to a defect in the mesh of the bulk. Nevertheless the detector proved to be really useful for checking the alignment of the neutron beam optics of the facility. Measurements with a new pixelized bulk detector for the determination of the beam interception factor are forseen before the end of 2012.

1. Introduction

The neutron time-of-flight (n_TOF) facility at CERN is a white neutron source based on spallation of 20 GeV/c proton beam with pulses 6 ns r.m.s. hitting a Pb target with a minimum repetition rate of 2.4 seconds. A 185 m long evacuated tube leads neutrons to an experimental area (EAR or EAR-1) equipped with several detectors for neutron-induced capture, fission and (n, α) cross sections. A detailed description of the facility can be found in [1].

Neutron-induced reaction measurements need an accurate knowledge of the incident flux. At n_TOF this is measured with a silicon monitor [2] and a Micro-mesh gaseous structure (micromegas) detector [3] of microbulk type [4], as well as a very accurate estimation of the spatial profile, determined with a micromegas detector of bulk type [5] in order to calculate the beam interception factor, i.e. the correction to be applied to the extracted neutron induced cross sections when the sample is smaller than the beam diameter. Micromegas detectors are a stack of one ionization chamber and one proportional chamber. A thin mesh separates the two communicating region, where two different electric fields are applied to obtain respectively the ionization and multiplication charge regimes. When the anode and the mesh of the detector are constructed into a single piece, this is called bulk. The main difference between bulks and microbulks is the thickness of the mesh, thinner in the latter thanks to the fabrication procedure.

2. Detector

The n_TOF beam profiler is a circular bulk of 4 cm radius with a typical bulk thickness of 128 μm. The readout is smaller than the anode itself and it is obtained by segmenting a square portion of 6 cm side of the anode in two orthogonal directions, called X and Y in the reference frame of the detector, by 106 strips. The detector allows therefore the determination of the beam image with a spatial resolution of 0.5 mm as a function of the time-of-flight. A 2 μm thick layer of BC_4 enriched in ^{10}B is deposited on the drift and acts as a neutron/charged particle converter through the $^{10}B(n,\alpha)^7Li$ reaction. The drift to mesh distance is 4 mm, and the detector is operated with and admixture of Ar (90 %), CF_4 (8 %) and C_4H_{10} (2 %). In order to reduce the number of channels necessary to collect the output of the strips and of the mesh, two gassiplex cards are employed.

3. Analysis

The analysis procedure consists in identifying signals caused by α particles or ^7Li particles produced by the interaction of neutrons with the converter and, for every interaction, associating to each strip of the detector its signal amplitude. The baseline level in each strip is determined through a measurement without beam, called pedestal run. The following step consists in subtracting, for each strip, the baseline level to the registered signals and identifying the strips with a leftover higher than a certain threshold. The set of these strips is called cluster and an algorithm to find the center of charge of each cluster is applied. By exploiting the time information of the mesh signal, a bi-dimensional histogram is filled with pairs of centers of charges calculated in the two orthogonal directions in time coincidence and the beam image is obtained as a function of time of flight. Since the axis of the detector are tilted of 135° with respect to the floor and walls of the experimental area, a rotation has to be applied to the beam image in order to visualize it in the reference system of the laboratory. A bi-dimensionnal Gaussian fit of the beam profile allows the study of its widths. In the end, the beam interception factor is extracted by calculating the ratio of the number of neutrons hitting the area covered by a sample to the number of neutrons in the whole beam.

4. Results

Data collected in the years 2009 - 2012 have been analyzed. In 2009 the study of the influence of the beam optics alignment on the beam profile was studied, allowing to detect a misalignment of the second collimator (Fig. 1).

A study of the gain of the detector showed that the distance between the mesh and the anode was not constant because of a slightly curved mesh plane, provoking differences in gain between different strips. This issue was partially solved by fitting experimental data to exclude the non operative strips. Nevertheless, given the fact that the problem concerns a large portion of the detector, it was not possible to totally correct for this.

Fig. 2 shows a comparison of the beam interception factor for a sample of 1 cm diameter obtained from simulations, from the measured data and from the Gaussian fit to the latter. Discrepancies between the results given by the fit to our data and simulations reach 12 %, but their trends are similar and in agreement with the expectations. Since the low energy neutrons are produced after several scatterings in the moderator of the spallation target (made of H_20), the neutron beam should be wider at low neutron energies than at high neutron energies, with the consequence that the beam interception factor increases with the neutron energy.

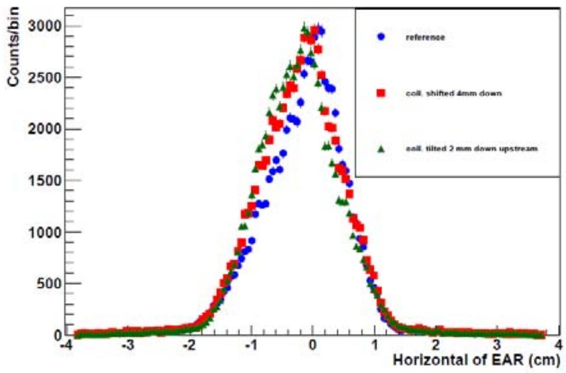

Fig. 1. Beam profile projected along the vertical axis in the reference system of the laboratory.

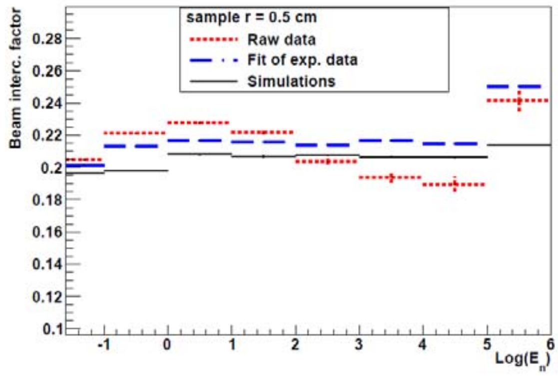

Fig 2. Beam interception factor for a sample of 1 cm diameter.

5. Conclusions

A study of the beam profile was performed at the n_TOF facility with a micromegas detector of bulk type. Thanks to these studies a misalignment of the second collimator was detected and corrected for. The trend of the extracted beam interception factor as a function of the incident neutron energy is in agreement with expectations, but always higher and discrepancies reach 12%. This is ascribed to a defect in the mesh of the detector and a measurement with a new pixelized micromegas detector of bulk type is already scheduled before the end of 2012.

REFERENCES

1. *The n_TOF Collaboration,* CERN n_TOF Facility: Performance Report // CERN/INTC-O-011, INTC-2002-037, CERN-SL-2002-053 ECT. - 2001.
2. *Marrone S. et al.* // Nuclear Instruments and Methods in Physics Research. - 2004. - Vol. A517. - P. 389 - 398.
3. *Giomataris Y., Rebourgeard Ph., Robert J.P., Charpak G.* Micromegas: a highgranularity position-sensitive gaseous detector for high particle-flux environments // Nucl. Instr. Meth. - 1996. - Vol. A376. - P. 29 - 35.
4. *Giomataris Y., De Oliveira R., Andriamonje S. et al.* Micromegas in a bulk // Nucl. Instr. Meth. - 2005. - Vol. A560. - P. 405 - 408.
5. *Andriamonje S., Attie D., Berthoumieux E. et al.* Development and performance of microbulk micromegas detectors // J. Instrum. - 2010. - Vol. 5. - P. 02001 - 02013.